Since January 2020 Elsevier has created a COVID-19 resource centre with free information in English and Mandarin on the novel coronavirus COVID-19. The COVID-19 resource centre is hosted on Elsevier Connect, the company's public news and information website.

VIROLOGY 166, 328–338 (1988)

Regional Localization of Virus in the Central Nervous System of Mice Persistently Infected with Murine Coronavirus JHM

STANLEY PERLMAN,*,[1] GARY JACOBSEN,* AND STEVEN MOORE†

*Departments of *Pediatrics and †Pathology, University of Iowa, Iowa City, Iowa 52242*

Received March 4, 1988; accepted June 8, 1988

Suckling C57BL/6 mice infected with mouse hepatitis virus strain JHM (MHV-JHM) develop either a fatal acute encephalomyelitis or a late onset demyelinating disease, depending on whether they are nursed by unimmunized or immunized dams. To determine the localization of virus-specific RNA, serial sections of brains from infected and uninfected mice were annealed with a ^{35}S-labeled antisense RNA probe and analyzed by film autoradiography. In the mice with acute encephalomyelitis, viral RNA was present in the mesencephalon, hypothalamus, hippocampus, basal ganglia, subcortical white matter, and thalamus. Viral RNA was detected in the spinal cords of all mice with the late onset, demyelinating encephalomyelitis, but was distributed into three different patterns in the brains of these mice, even though all had the same clinical disease. In the first group, viral RNA was detected only in the brainstem. In the second group, viral RNA was detected in the brainstem, thalamus, and cerebral grey matter. This distribution was consistent with viral spread along well-defined tracts connecting these parts of the brain. In the third group, viral RNA could be detected both in the brainstem and in several white matter tracts within close physical proximity to the optic chiasm. This distribution was consistent with viral spread by an extracellular route from one white matter tract to other tracts which were physically close, but which were not part of the same pathways. These results suggest that MHV-JHM spreads through the central nervous system both along well-defined neuronal pathways and by spread from contiguous structures, but also suggest that viral replicates preferentially in a limited number of areas of the brain. The technique of *in situ* hybridization with film autoradiography should be generally useful for analyzing macroscopic movements of virus within infected organs. © 1988 Academic Press, Inc.

INTRODUCTION

The JHM strain of mouse hepatitis virus, a member of the Coronavirus family, causes acute, subacute, and chronic neurological infections in mice and rats. Suckling mice and rats are susceptible to an invariably fatal acute encephalomyelitis characterized by widespread destruction of grey and white matter. Neuronal destruction is believed to be a major component of this disease entity, with minimal demyelination noted on necropsy. On the other hand, the acute and chronic demyelinating diseases are characterized by widespread demyelinating lesions, with minimal involvement of neurons, but extensive infection of oligodendrocytes and astrocytes (Cheever *et al.*, 1949; Lampert *et al.*, 1973; Weiner, 1973; Herndon *et al.*, 1975; Nagashima *et al.*, 1978, 1979; Sorensen *et al.*, 1980; Stohlman and Weiner, 1981; Siddell *et al.*, 1983).

The acute encephalomyelitis, but not the demyelinating disease, can be prevented by use of attenuated virus (temperature-sensitive mutants), by selection of neutralization-resistant virus with monoclonal antibody prior to administration into the mouse, by infusion with neutralizing antibody prior to inoculation, or by suckling of infected mice by immunized dams (Haspel *et al.*, 1978; Buchmeier *et al.*, 1984; Pickel *et al.*, 1985; Fleming *et al.*, 1986; Dalziel *et al.*, 1986; Perlman *et al.*, 1987).

When C57BL/6 suckling mice are nursed by immunized dams and inoculated with MHV-JHM, they are completely protected against the acute encephalomyelitis; however, 40–90% of these mice develop a late onset, symptomatic demyelinating disease at 3–8 weeks p.i. Clinically, this disease is characterized by hindlimb paralysis, with minimal signs of acute encephalitis (signs of encephalitis include hunching, ruffled fur, irritability). Virus can be cultured primarily from symptomatic mice, but viral antigen can be detected in most mice, whether symptomatic or not (Perlman *et al.*, 1987). A similar symptomatic demyelinating disease has been described in rats (Nagashima *et al.*, 1978; Sorenson *et al.*, 1980; Parham *et al.*, 1986).

All mice, whether nursed by immunized or unimmunized dams, have histological evidence of diffuse encephalomyelitis at 5–7 days p.i., suggesting that viral RNA might be present in multiple sites in the brain at this time. In order to understand the pathogenesis of viral persistence and late onset clinical disease in the offspring of the immunized dams, it is important to determine the relationship between the sites of viral repli-

[1] To whom requests for reprints should be addressed.

0042-6822/88 $3.00

cation in asymptomatic mice at 5–7 days p.i. and in those with hindlimb paralysis. In the simplest model, viral RNA would be detected in the same regions of the CNS in both cases, suggesting that clinical disease resulted from viral replication at all the initial sites of viral infection.

In order to determine the sites of viral replication, we have used the technique of *in situ* hybridization with specific ^{35}S-labeled antisense RNA probes (Cox *et al.,* 1984) and analysis by film autoradiography. This method allows rapid examination of serial sections of brains and accurate determination of gross patterns of RNA accumulation. Using this technique, we have analyzed brains and spinal cords from mice exhibiting either the acute encephalomyelitis or the late onset demyelinating encephalomyelitis for the presence of viral RNA.

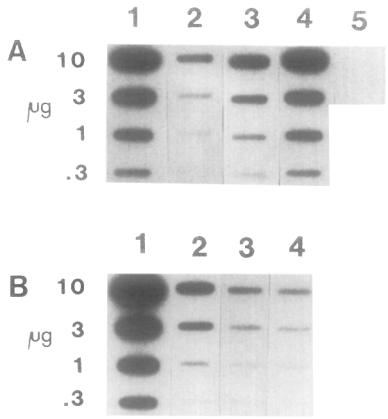

FIG. 1. Slot blot analysis of RNA from infected and uninfected samples. RNA was extracted from the brains and spinal cords of infected mice and from uninfected L-2 tissue culture cells. Blots were prepared, hybridized with ^{32}P-labeled antisense RNA probe, processed, and quantitated with a Shimadzu C-930 densitometer. The amounts of each RNA applied to the filter are shown at the left. (A) RNA from brain (lane 1) and spinal cord (lane 2) of mouse with acute encephalomyelitis (5 days p.i.), from brain (lane 3) and spinal cord (lane 4) of mouse with hindlimb paralysis (32 days p.i.), and from uninfected L-2 cells (lane 5). In this experiment, viral RNA was concentrated in the brain 50-fold compared to in the spinal cord in the acutely infected mouse, whereas the spinal cord of the mouse with hindlimb paralysis was 4.5-fold enriched in viral sequences as compared to the brain. (B) RNA from brain (lane 1) and spinal cord (lane 2) of mouse with acute encephalomyelitis (5 days p.i.) and from brain (lane 3) and spinal cord (lane 4) of maternal antibody-protected mouse (5 days p.i.).

MATERIALS AND METHODS

Animals

Pathogen-free C57BL/6 mice, purchased from Jackson Laboratories, were immunized with MHV-JHM and the offspring were inoculated intranasally with 6×10^4 PFU MHV-JHM in 10 μl at 10 days of age.

Virus and cells

MHV-JHM, obtained from Dr. Susan Weiss, University of Pennsylvania, was grown and titered as previously described (Perlman, *et al.,* 1987).

MHV DNA clones

Clone g344, obtained from Dr. Susan Weiss, includes genes 5 and 6 and 200 nucleotides of genes 4 and 7 of mouse hepatitis virus, strain A59 (MHV-A59) (Budzilowicz *et al.,* 1985). In preliminary experiments, we determined that this probe would readily anneal to intracellular RNA isolated from MHV-JHM-infected cells under stringent conditions of annealing. For the experiments described below, the insert from this clone was subcloned into a vector containing the SP6 promoter (pSP 18) and a clone with the insert in the antisense orientation was selected. Radioactive antisense RNA was synthesized using SP6 polymerase by standard procedures (Melton *et al.,* 1984) except that either [^{32}P]UTP or [^{35}S]UTP was mixed with unlabeled UTP to give a final concentration of 12 μM. Specific activity of the resultant RNA was $1–2 \times 10^9$ dpm/μg.

Blot hybridization

RNA was isolated from the brains and spinal cords of infected and uninfected mice using the guanidine isothiocyanate method (Maniatis *et al.,* 1982). RNA was also isolated from uninfected and infected L-2 tissue culture cells. All RNAs were shown to be intact by formaldehyde–agarose gel electrophoresis. For blot analysis, RNA was prepared and applied to nitrocellulose paper as previously described (Perlman *et al.,* 1986). Prehybridization was performed in 50% formamide, 50 m*M* phosphate buffer, 5× SSC (1× SSC is 0.15 *M* NaCl, 0.015 *M* Na citrate), 0.1% sodium dodecyl sulfate, 1 m*M* EDTA, 250 μg/ml sonicated and denatured salmon sperm DNA, and 5× Denhardt's solution (50× Denhardt's solution is 1% bovine serum albumin, 1% Ficoll, and 1% polyvinylpyrrolidone) at 60°. Hybridization was performed in the same solution, with addition of $1–2 \times 10^6$ dpm/ml of ^{32}P-labeled RNA probe. Filters were washed sequentially with (1) 0.75 *M* NaCl, 0.15 *M* Tris, pH 7.6, 10 m*M* EDTA, 0.025 *M* Na*P*i buffer and 0.1% SDS for 1 hr at 68°; (2) 0.15 *M* NaCl, 0.03 *M* Tris, pH 7.6, 2 m*M* EDTA, 0.025 *M* Na*P*i buffer, 1× Denhardt's solution for 1 hr at 68°; (3) 0.05 *M* NaCl, 5 m*M* Tris, pH 7.6, 0.4 m*M* EDTA, 0.1% SDS for 1 hr at 68°; (4) 2× SSC 5 min at room temperature repeated twice; (5) 2× SSC containing ribonuclease A (1 μg/ml) for 15 min at room temperature; (6) 2× SSC for 5 min at room temperature.

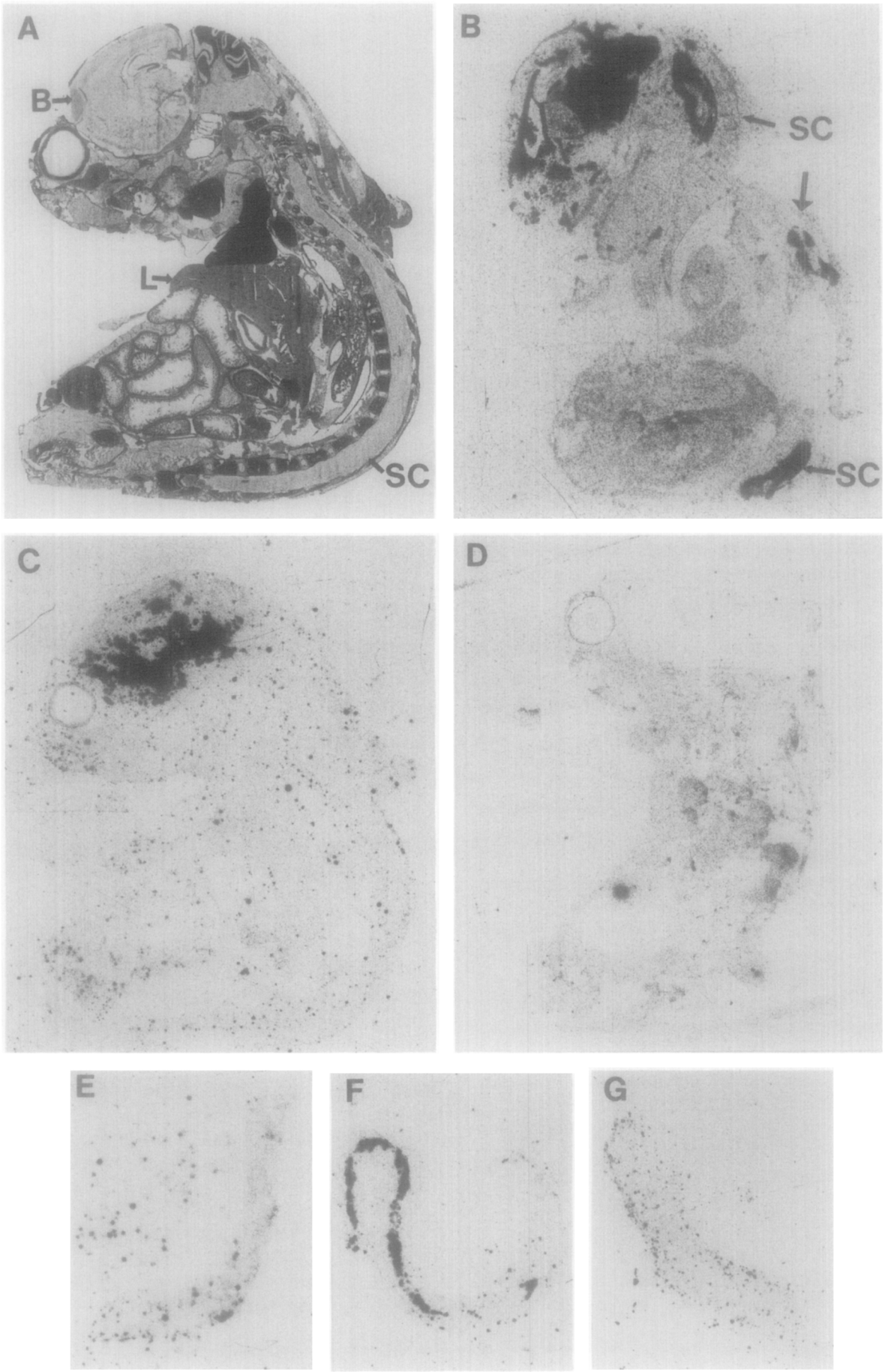
A
B
L
SC
B
SC
SC
C
D
E
F
G

Blots were developed by exposure to Kodak XAR-5 film at −70° and autoradiographs were quantitated with Shimadzu C-930 densitometer.

In situ hybridization

Mice were perfused with phosphate-buffered saline (PBS) via intracardiac puncture. Isolated brains and spinal cords or whole mice were embedded in Tissue-Tek II O.C.T. medium (Miles Laboratory and frozen in ethanol/dry ice. Eighteen micrometer sections were prepared at 170 to 200 μm intervals (35–45 sections were cut per brain analyzed) and fixed with PLP fixative (2% paraformaldehyde, 0.075 *M* lysine, 0.01 *M* sodium periodate, and 0.037 *M* phosphate buffer, pH 7.5) (McLean and Nakane, 1974) onto acid-washed, acetylated glass slides which had been treated with Denhardt's solution (Haase *et al.,* 1984). Five to six sections were placed per slide. *In situ* hybridization was performed by a modification of the method of Cox *et al.* (1984). Sections were pretreated with proteinase K at a final concentration of 1 μg/ml in 0.1 *M* Tris, pH 8, 0.05 *M* EDTA for 20 min at 37° and then with acetic anhydride (0.25% (v/v) in 0.1 *M* triethanolamine) for 10 min at room temperature. Slides were then dehydrated in graded ethanol solutions prior to hybridization.

In situ hybridization was performed in a solution containing 50% formamide, 1× Denhardt's solution, 0.3 *M* NaCl, 20 m*M* Tris, pH 7.6, 5 m*M* EDTA, 10 m*M* dithiothreitol, and 100 μg/ml yeast tRNA overnight at 45° with radioactive antisense probe. ^{35}S-Labeled RNA was generated as described above and degraded to about 100 nucleotides (Cox *et al.,* 1984). Approximately 1–2 × 10^6 cpm was used per slide; use of greater amounts of probe increased the background radioactivity on the final autoradiograph to unacceptably high levels. Siliconized coverslips were sealed with rubber cement.

After annealing, coverslips were removed and slides were washed three times with 4× SSC, 0.1 m*M* DTT at room temperature for 5 min, rinsed with water, and air dried. Slides were treated with RNase (20 μg/ml) in 0.5*M* NaCl, 0.01 *M* Tris, pH 7.5, 0.1 m*M* DTT at 37° for 30 min, and in the same buffer without enzyme for 30 min at 37°. Finally, slides were washed with 2× SSC, 0.1 m*M* DTT for 30 min at room temperature, 1× SSC, 0.1 m*M* DTT for 10 min at 50°, and 1× SSC, 0.1 m*M* DTT for 15 min at room temperature. Slides were rinsed with water and air dried. Slides were initially exposed to X-ray film (Kodak XAR) for 1–3 days at 4° and then dipped in NTB-3 nuclear emulsion prior to exposure for 1–2 weeks at 4°. Slides were stained with hematoxylin prior to examination by light microscopy.

RESULTS

Analysis of infected brains and spinal cords by blot hybridization

Young C57BL/6 mice inoculated intranasally with MHV-JHM and suckled by unimmunized dams show little evidence of histological change in the CNS at 3 days p.i., but by 5 days p.i., perivenous, parenchymal, and leptomeningeal inflammatory cellular infiltrates and extensive areas of necrosis are apparent in both grey and white matter. Glial stars (proliferating astrocytes and microglia surrounding neurons) are also apparent in the brains of these mice. All of these mice are dead by 7 days p.i.

Suckling mice nursed by immunized dams and inoculated with the same amount of MHV-JHM, although asymptomatic, also show evidence of encephalomyelitis on histological examination at 5–7 days p.i., with extensive lymphocytic cellular infiltrates present throughout the grey and white matter. Glial stars are evident in the cerebral cortex. MHV-JHM can only occasionally be cultured at low titer from the brains but not the spinal cords of these mice. By 14 days p.i., the brains show significantly less evidence of encephalitis, with only a few areas of lymphocytic infiltration present in the parenchyma. At 4–6 weeks p.i., 40–90% of these mice developed hindlimb paralysis, with lymphocytic infiltration and necrosis most prominent in the white matter of the brainstem and spinal cord. Inflammatory cellular infiltrates are also present in the adjacent grey matter, particularly in the brainstem (Perlman *et al.,* 1987).

To determine the pattern of accumulation of viral RNA in mice with clinical disease, RNA was prepared from the brains and spinal cords of mice with acute encephalomyelitis (5 days p.i.) and from those of mice protected by maternal antibody at either early times p.i.

FIG. 2. Localization of viral RNA in whole infected mice. Sections from an uninfected mouse, from a mouse with acute encephalomyelitis, and from a mouse with hindlimb paralysis were prepared and annealed with ^{35}S-labeled RNA probe as described under Materials and Methods. Sections were also prepared from spinal cords of mice with the same clinical diseases. (A) Section from whole mouse with acute encephalomyelitis (5 days p.i.) stained with hematoxylin and eosin. (B) Autoradiograph of whole mouse with hindlimb paralysis (26 days p.i.); only rostral and caudal portions of the spinal cord appear in the plane of the section. (C) Autoradiograph of mouse shown in (A). (D) Autoradiograph of uninfected whole mouse. (E–G) Autoradiographs of isolated spinal cords from mouse with acute encephalomyelitis (5 days p.i.) (E), mouse with hindlimb paralysis (47 days p.i.) (F), uninfected mouse (G). B, brain; SC, spinal cord; L, liver.

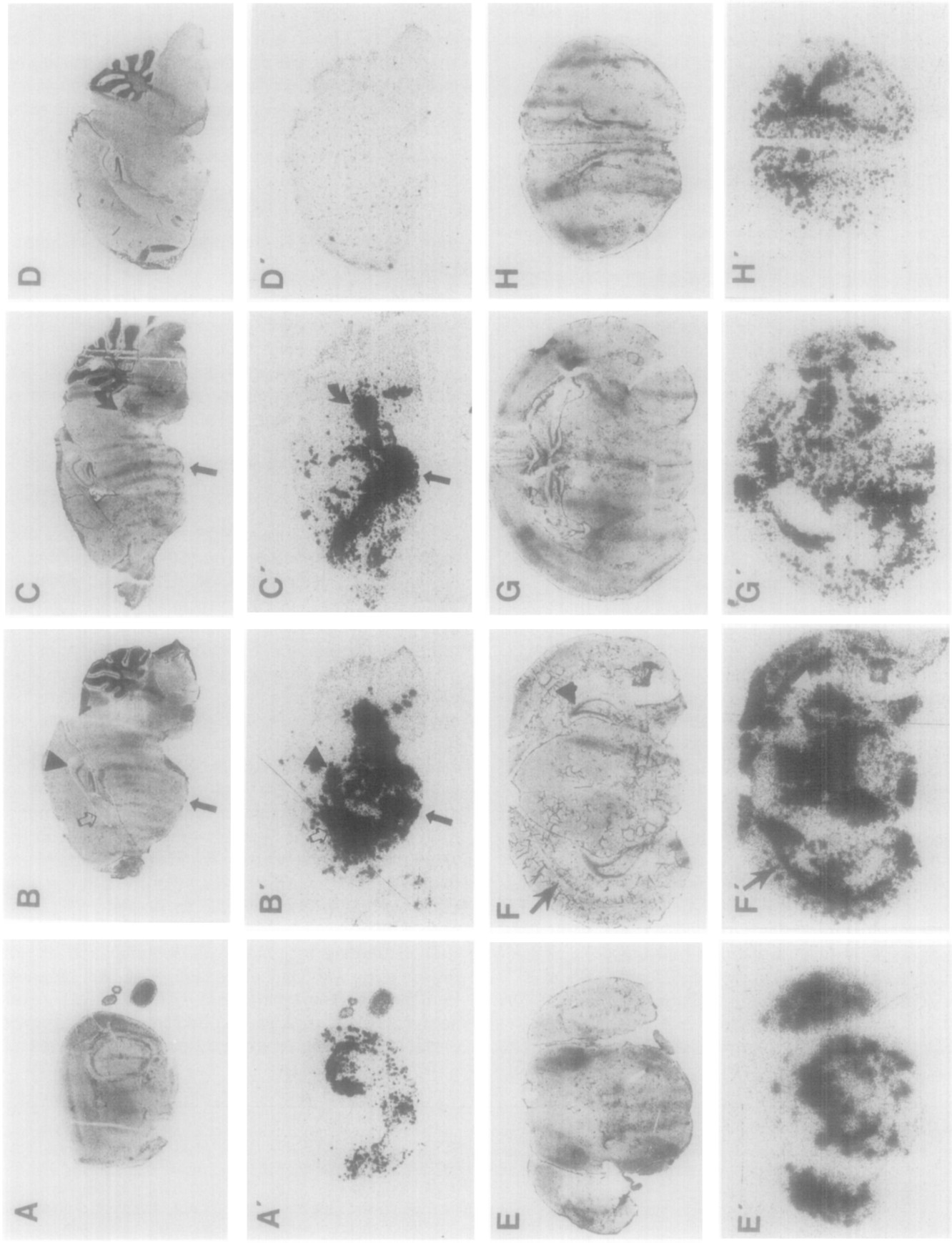
A
A'
B
B'
C
C'
D
D'
E
E'
F
F'
G
G'
H
H'

(5 days p.i.) or after the development of hindlimb paralysis (4–8 weeks p.i.). After fixation to nitrocellulose filters, the samples were annealed with a ^{32}P-labeled antisense RNA probe, synthesized as described under Materials and Methods, which will anneal to all intracellular and extracellular species of MHV-JHM RNA. The probe, as expected, did not anneal to RNA isolated from uninfected tissue culture cells (Fig. 1) or uninfected brains (not shown).

As shown in Fig. 1, approximately 30- to 50-fold more virus-specific RNA was present in the brain per microgram of RNA than in the spinal cord of mice with acute encephalomyelitis, consistent with the clinical and histological findings discussed above. The brains of mice protected by maternal antibody at early times p.i. contained approximately 1% as much virus-specific RNA as did those mice with the acute encephalomyelitis, although the concentration of MHV-JHM RNA in the brains of these asymptomatic mice was only 1–3 times that of the spinal cords. In mice with hindlimb paralysis, the concentration of MHV-JHM RNA in the spinal cord was one-half to five times the concentration of RNA in the brain, consistent with the greater involvement of the spinal cord both clinically and on histological examination in these mice.

Analysis of whole mice by *in situ* hybridization

To localize further MHV-JHM RNA, frozen sections from whole uninfected and infected mice with either acute encephalomyelitis or hindlimb paralysis were analyzed by *in situ* hybridization and autoradiography as described under Materials and Methods. As expected, no annealing occurred with any tissue from uninfected mice (Fig. 2D) whereas the brains from mice with either acute encephalomyelitis (Fig. 2C) or hindlimb paralysis (Fig. 2B) annealed with the probe. Viral RNA was detected in the spinal cord of mice with hindlimb paralysis (Fig. 2B). Similarly viral RNA was detected in isolated spinal cords from mice with hindlimb paralysis (Fig. 2F) but not from uninfected mice (Fig. 2G) or from infected mice with acute encephalomyelitis (Fig. 2E). These results were consistent with those obtained in the blot analysis described above (Fig. 1).

Analysis of serial brain sections by *in situ* hybridization

Viral RNA was localized more precisely by hybridization of probe to serial sagittal, coronal, or transverse sections of brains from unprotected mice with acute encephalomyelitis or from maternal-antibody protected mice either early after infection or after development of hindlimb paralysis.

No annealing occurred with sectioned brains from uninfected mice (Fig. 3D′), whereas viral RNA could readily be detected in sections from the brains of mice with acute encephalomyelitis at 5 days p.i. (Figs. 3A′–C′, E′–H′). Most portions of the brains of these mice contained viral RNA, although viral sequences were most concentrated in the subcortical white matter, the thalamus, the basal ganglia, the hippocampus, the hypothalamus, and the mesencephalon. Microscopic examination of these sections showed that viral RNA was most concentrated in areas with widespread inflammatory cell infiltration. As expected from previous histological results, no viral RNA was detected in the cerebellum of these infected mice (Bailey *et al.*, 1949). Each of the brains examined (7/7) gave the same pattern of viral RNA expression.

Suckling mice nursed by immunized dams showed evidence of diffuse encephalomyelitis upon histological examination at 7 days p.i. although they were asymptomatic (Perlman *et al.*, 1987). When the brains of such mice were analyzed by *in situ* hybridization, viral RNA could be detected only in the mesencephalon and pons and, occasionally, in the white matter of the cerebellum (Fig. 4B). The distribution of labeling suggested preferential accumulation of viral RNA in the brainstem, even though histological evidence of encephalitis was present elsewhere.

Mice which subsequently developed hindlimb paralysis exhibited three different patterns of viral RNA expression, even though the mice had indistinguishable clinical diseases. In the first pattern, present in 6 of the 13 mice analyzed, viral RNA could be detected only in the brainstem (Figs. 4C and 5A–D). As shown in Fig. 4C, when sagittal sections of these brains were examined, the pattern of viral RNA accumulation was very similar to the results seen when the mice were analyzed at a few days after inoculation (Fig. 4B). Examina-

FIG. 3. Localization of viral RNA in brains of mice with acute encephalomyelitis. Serial sections were prepared from uninfected mice and from mice with acute encephalomyelitis (5 days p.i.) and annealed with a ^{35}S-labeled RNA probe. No annealing occurred with any section from uninfected mice. A representative section is shown in (D) and its autoradiograph in (D′). Sagittal (A–C) and coronal (E–H) sections were prepared from the brains of mice with acute encephalomyelitis. (A–C) Hematoxylin-stained sagittal sections, lateral (A) to medial (C). (A′–C′) Autoradiographs of these sections. Straight arrow, hypothalamus; curved arrow, mesencephalon; open arrow, basal ganglia; arrowhead, hippocampus. (E–H) Hematoxylin-stained coronal sections, caudal (mesencephalon) to rostral (cerebrum). (E′–H′) Autoradiographs of these sections. Arrow, subcortical white matter; arrowhead, hippocampus.

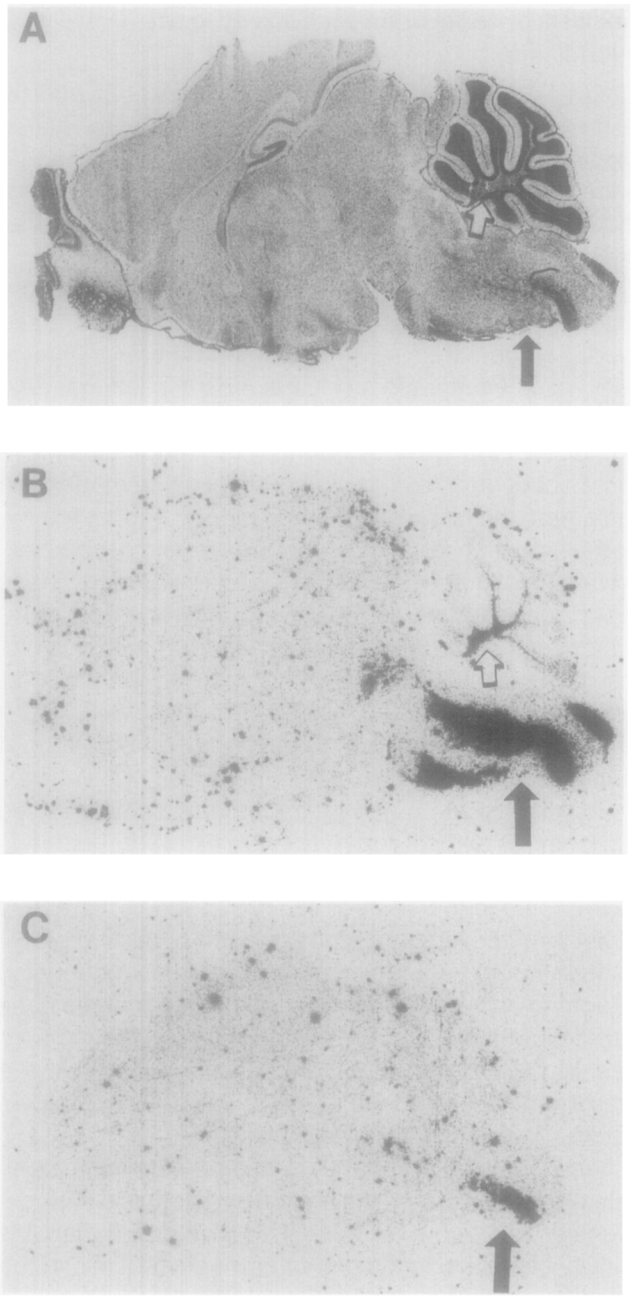

FIG. 4. Sagittal sections of antibody-protected mice. (A) Hematoxylin stain and (B) autoradiograph of mid-sagittal section from asymptomatic mouse at 6 days p.i. Viral RNA is detected only in the brainstem (solid arrow) and the cerebellar white matter (open arrow). (C) Autoradiograph of mid-sagittal section from mouse with hindlimb paralysis (29 days p.i.). Viral RNA is detected only in brainstem (arrow).

tion of coronal sections revealed the presence of viral sequences predominantly in the ventral aspects of the brainstem (Figs. 5A–C), with little or no viral RNA detected in other portions of the brain (Fig. 5D).

In the second pattern, observed in 4 of 13 mice, viral RNA was present in the brainstem as before (Figs. 5E–F), but was also present in the thalamus (Fig. 5G) and cerebral cortex (Figs. 5G–H).

In the third pattern, present in 3 of 13 infected mice, viral RNA was also present in the brainstem (Figs. 6A–D); however, viral RNA could be detected in several coronal sections at the level of the optic chiasm. As shown in Figs. 6G–I, viral RNA was not only present in the optic chiasm, but could also be detected in several nearby white matter tracts, including the fornix and the corpus callosum. MHV-JHM RNA was also detected in the basal ganglia, with preferential labeling of the white matter tracts which transverse this structure. In contrast to the results obtained with the second set of mice, viral RNA could not be detected in the cerebral grey matter or in the thalamus.

In all the brains analyzed, microscopic examination of the sections showed that viral RNA was detected in areas with extensive inflammatory cellular infiltrates.

No obvious correlation could be detected between the pattern of RNA accumulation and either the age of onset of hindlimb paralysis or the number of days between the onset of paralysis and the sacrifice of the mouse.

DISCUSSION

We have determined the location of viral RNA within infected brains by *in situ* hybridization. At 5–7 days p.i., the asymptomatic offspring of immunized dams and the acutely ill offspring of unimmunized dams both show histological evidence of acute, diffuse encephalitis with inflammatory cellular infiltrates and areas of necrosis (Bailey *et al.*, 1949; Weiner, 1973; Perlman *et al.*, 1987). The patterns of viral RNA accumulation were different, however, between the asymptomatic and symptomatic mice at these early times p.i. and correlated with the clinical symptomatology: viral RNA was detected in many portions of the brain in the symptomatic mice (Fig. 3) but was restricted primarily to the brainstem of the asymptomatic mice (Fig. 4). In both cases, however, viral RNA was localized to areas with extensive inflammatory changes.

A large fraction of these asymptomatic mice developed hindlimb paralysis 3–8 weeks p.i., with accumulation of viral RNA in the brainstem and spinal cord of all mice as well as in other portions of the brain in some mice. The distribution of viral RNA corresponded to the sites of maximal inflammatory response and necrosis. This result suggests that the brainstem is a site of initial infection and also an important site for persistence and, ultimately, amplification in the mice that develop hindlimb paralysis. In turn, this clinical sign is most likely the consequence of preferential viral replication

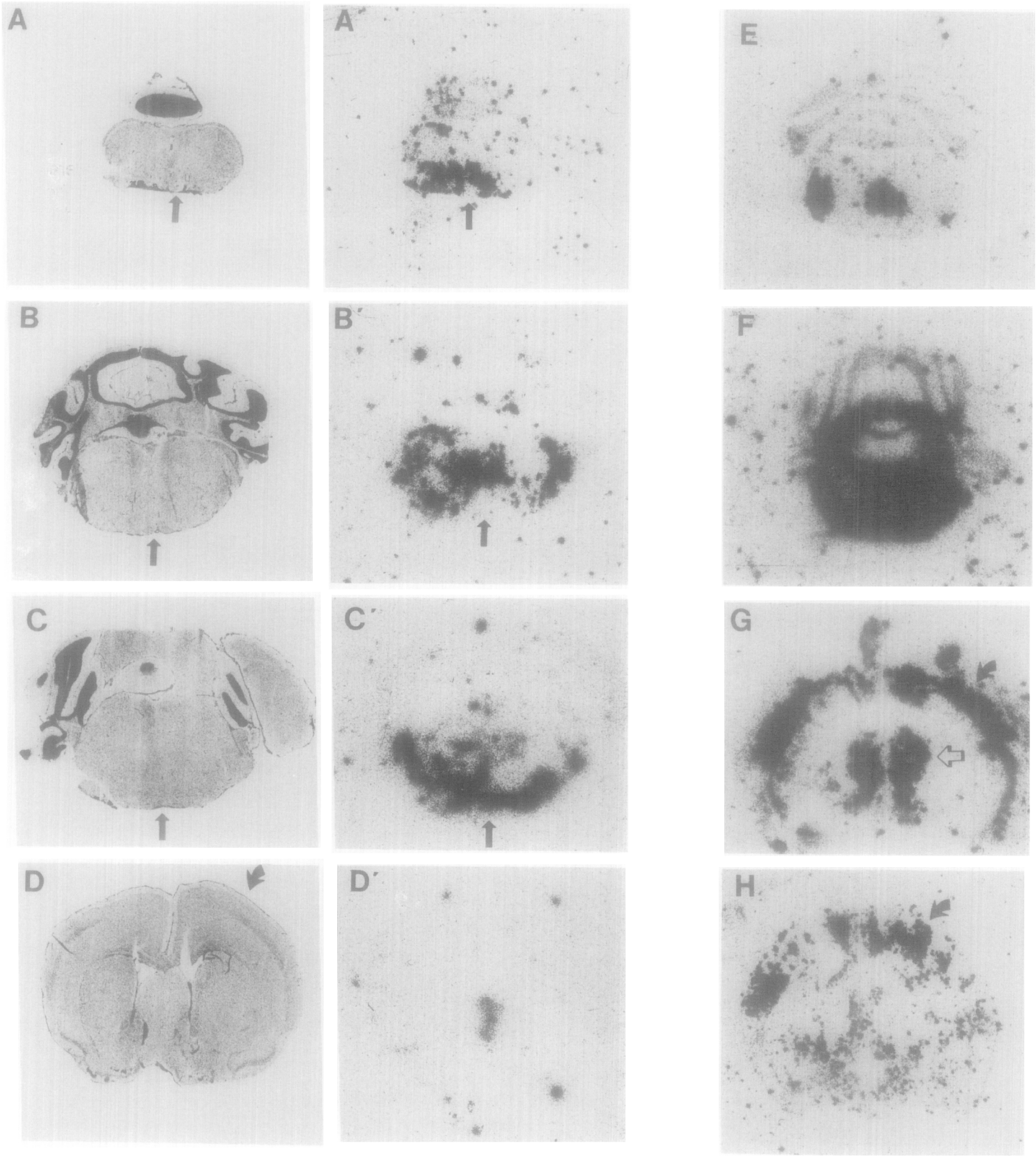

FIG. 5. Coronal sections of antibody-protected mice with hindlimb paralysis. (A–D and A′–D′) Hematoxylin stain and autoradiograph of coronal sections from mouse (30 days p.i.) with viral RNA detected only in brainstem. (A–C, A′–C′) Section from brainstem region. (D) Section from level of basal ganglia. (E–H) Coronal sections from brain of mouse (47 days p.i.) with labeling confined to brainstem (E, F), thalamus (G), and cerebral grey matter (G, H). Sections oriented caudal to rostral (A–D, A′–D′, E–H). Straight arrow, brainstem; curved arrow, cerebral grey matter; open arrow, thalamus.

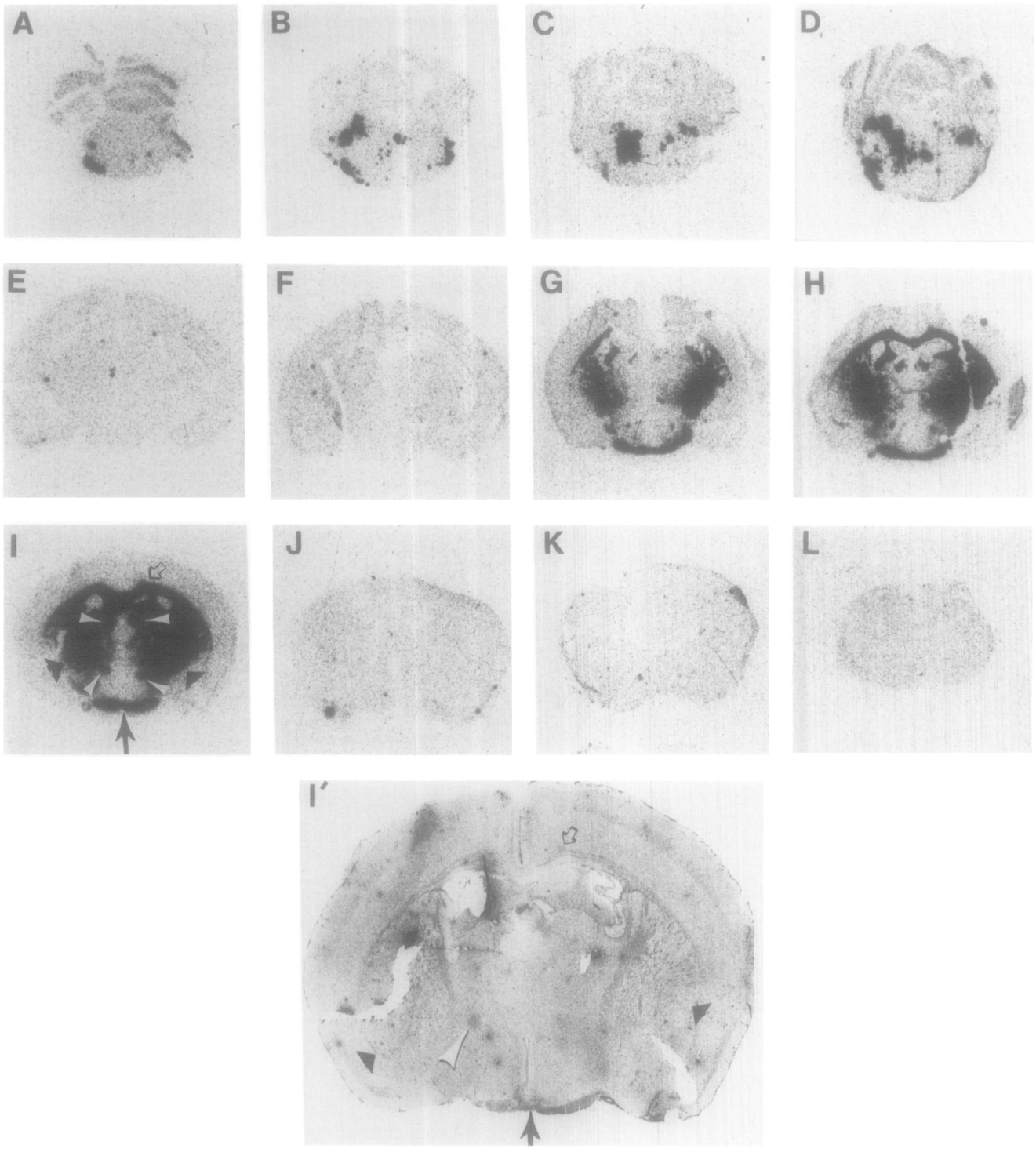

FIG. 6. Coronal sections of hindlimb paralyzed mice. Serial sections (caudal (A) to rostral (L)) from mouse (25 days p.i.) with labeling confined to brainstem, optic chiasm, fornix, corpus callosum, and basal ganglia. (A–D) Brainstem region. (G–I) Sections at level of optic chiasm. Note lack of labeling on slices caudal (E, F) and rostral (J–L) to basal ganglia. (I') Hematoxylin stain of section (I). Solid arrow, optic chiasm; solid arrowhead, basal ganglia; open arrowhead, fornix; open arrow, corpus callosum.

in this part of the CNS and in the spinal cord. In mice with acute demyelination caused by MHV-JHM, inflammatory cellular infiltrates, and patchy demyelinating lesions are particularly prominent in the brainstem and spinal cord (Lampert *et al.,* 1973), consistent with our results.

The results suggest that MHV-JHM may spread within the CNS both to adjacent areas and to distant sites along well-defined neuronal pathways. In the acute encephalomyelitis, viral RNA can be detected throughout the mesencephalon, the thalamus, the basal ganglia, the hippocampus, the hypothalamus, and the subcortical white matter. These structures are all in close proximity, and virus at high titer can be isolated from mice with this clinical disease. This suggests that viral spread is predominantly to contiguous areas with rapid and simultaneous destruction of many portions of the brain.

In contrast, Lavi *et al.,* (1988) showed, using immunohistochemical techniques to detect viral antigen, that in the acute, relatively mild encephalomyelitis caused by MHV-A59, virus spread through the olfactory bulbs to associated structures of the limbic system. They concluded that virus spread via well-defined CNS pathways in this case.

Spread of MHV-JHM may be to both contiguous and distant areas in mice with the late onset demyelinating disease. At early times after inoculation, viral RNA can be detected primarily in the ventral brainstem where many cranial nerve nuclei are located. One explanation for this observed distribution may be MHV-JHM spread centripetally to the brainstem through peripheral nerves. Alternatively, virus may reach the brainstem via viral invasion of the olfactory bulb and limbic system with spread from the latter to the midbrain tegmentum (Nauta and Domesick, 1981).

Three patterns of viral RNA expression were observed when these mice develop clinical disease. In all cases, viral RNA was present in the ventral brainstem, at approximately the same location as in the mice analyzed a few days after inoculation. This result suggests that the brainstem not only is the site of primary viral replication, but also is the source for viral spread, including caudal progression to the spinal cord. In the first pattern, MHV-JHM RNA was detected only in the brainstem. In the second pattern, MHV-JHM was also present in the thalamus and cerebral grey matter, consistent with cell to cell transmission of virus from the brainstem to the thalamus and cerebrum via the corticospinal, corticopontine, spinothalamic, and corticothalamic tracts and the medial lemniscus. An alternative explanation is that viral replication may occur independently in each of these regions.

In the third pattern of viral gene expression, viral RNA was detected in the brainstem and in the part of the brain physically adjacent to the optic chiasm. Several white matter tracts (optic chiasm, fornix, corpus callosum, and white matter of the basal ganglia) in this latter part of the brain contained viral RNA whereas other areas of the CNS associated with each of these entities (e.g., the hippocampus and mammillary bodies with the fornix) did not. This suggests that virus reactivated in one of these white matter tracts, such as the optic chiasm, and spread to other white matter tracts in close physical proximity. Alternatively, virus could have reactivated in the brainstem, with transport to this region by connecting tracts such as the pallidotegmental fibers (connecting brainstem and basal ganglia). Previous studies have indicated that demyelinating lesions in the optic chiasm are prominent in MHV-JHM-infected rats with demyelinating encephalomyelitis (Nagashima *et al.,* 1978; Sorensen *et al.,* 1980).

Regional localization by *in situ* hybridization and film autoradiography will be a useful technique for determining the location of virus in an infected brain as a function of time. Using this method with mice at different stages of development of clinical disease, it should be straightforward to determine the three-dimensional localization of virus at each time (Shepherd *et al.,* 1984) and from that, map the movement of virus during disease progression.

ACKNOWLEDGMENTS

We thank Drs. C. M. Stoltzfus, M. Dailey, and A. L. Olson for helpful discussions. This research was supported by NIH Grant R01 NS24401.

REFERENCES

BAILEY, O. T., PAPPENHEIMER, A. M., CHEEVER, F. S., and DANIELS, J. B. (1949). A murine virus (JHM) causing disseminated encephalomyelitis with extensive destruction of myelin. II. Pathology. *J. Exp. Med.* **90,** 195–212.

BUCHMEIER, M. J., LEWICKI, H. A., TALBOT, P. J., and KNOBLER, R. L. (1984). Murine hepatitis virus-4 (strain JHM)-induced neurological disease is modulated *in vivo* by monoclonal antibody. *Virology* **132,** 261–70.

BUDZILOWICZ, C. J., WILCZYNSKI, S. P., and WEISS, S. R. (1985). Three intergenic regions of coronavirus mouse hepatitis virus strain A59 genome RNA contain a common nucleotide sequence that is homologous to the 3′ end of the viral mRNA leader. *J. Virol.* **53,** 834–840.

CHEEVER, F. S., DANIELS, J. B., PAPPENHEIMER, A. M., and BAILEY, O. T. (1949). A murine virus (JHM) causing disseminated encephalomyelitis with extensive destruction of myelin. *J. Exp. Med.* **90,** 181–194.

COX, K. H., DELEON, D. V., ANGERER, L. M., and ANGERER, R. C. (1984). Detection of mRNAs in sea urchin embryos by *in situ* hybridization using asymmetric RNA probes. *Dev. Biol* **101,** 485–502.

DALZIEL, R. G., LAMPERT, P. W., TALBOT, P. J., and BUCHMEIER, M. J. (1986). Site-specific alteration of murine hepatitis virus type 4 peplomer glycoprotein E2 results in reduced neurovirulence. *Virology* **59,** 462–471.

FLEMING, J. O., TROUSDALE, M. D., EL-ZAATARI, F. A. K., STOHLMAN, S. A., and WEINER, L. P. (1986). Pathogenicity of antigenic variants of murine coronavirus JHM selected with monoclonal antibodies. *Virology* **58,** 869–875.

HAASE, A., BRAHIC, M., STOWRING, L., and BLUM, H. (1984) Detection of viral nucleic acids by in situ hybridization. *In* "Methods in Virol-

ogy" (K. Maramorosch, and H. Koprowski, Eds.), Vol. 7, pp. 189–226. Academic Press, New York.

HASPEL, M. V., LAMPERT, P. W., and OLDSTONE, M. B. A. (1978). Temperature-sensitive mutants of mouse hepatitis virus produce a high incidence of demyelination. *Proc. Natl. Acad. Sci. USA* **75,** 4033–4036.

HERNDON, R. M., GRIFFIN, D. E., MCCORMICK, V., and WEINER, L. P. (1975). Mouse hepatitis virus-induced recurrent demyelination. *Arch. Neurol* **32,** 32–35.

LAMPERT, P. W., SIMS, J. K., and KNIAZEFF, A. J. (1973) Mechanism of demyelination in JHM virus encephalomyelitis. *Acta Neuropathol.* **24,** 76–85.

LAVI, E., FISHMAN, P. S., HIGHKIN, M. K., and WEISS, S. R. (1988). Limbic encephalitis after inhalation of a murine coronavirus. *Lab. Invest.* **58,** 31–36.

MANIATIS, T., FRITSCH, E. F., and SAMBROOK, J. (1982). "Molecular Cloning: A Laboratory Manual." Cold Spring Harbor Laboratory, Cold Spring Harbor, NY.

MCLEAN, I. W., and NAKANE, P. K. (1974). Periodate–lysine–paraformaldehyde fixative: A new fixative for immunoelectron microscopy. *J. Histochem. Cytochem.* **22,** 1077–1083.

MELTON, D. A., KRIEG, P. A., REBAGLIATI, M. R., MANIATIS, T., ZINN, K., and GREEN, M. R. (1984). Efficient in vitro synthesis of biologically active RNA and RNA hybridization probes from plasmids containing a bacteriophage SP6 promoter. *Nucleic Acids Res.,* **12,** 7035–7056.

NAGASHIMA, K., WEGE, H., MEYEREMANN, R., and TER MEULEN, V. (1978). Coronavirus induced subacute demyelinating encephalomyelitis in rats: A morphological analysis. *Acta Neuropathol.* **44,** 63–70.

NAGASHIMA, K., WEGE, R., MEYERMANN, R., and TER MEULEN, V. (1979). Demyelinating encephalomyelitis induced by long term coronavirus infection in rats. *Acta Neuropathol.* **45,** 205–213.

NAUTA, W., and DOMESICK, V. B. (1981). Ramifications of the limbic system. *In* "Psychiatry and the Biology of the Human Brain" (S. Matthysse, Ed.), pp 165–188. Elsevier, New York.

PARHAM, D., TEREBA, A., TALBOT, P. J., JACKSON, D. P., and MORRIS, V. L. (1986). Analysis of JHM central nervous system infections in rats. *Arch. Neurol.* **43,** 702–708.

PERLMAN, S., RIES, D., BOLGER, E., LUNG-JI, C., and STOLTZFUS, C. M. (1986). MHV nucleocapsid synthesis in the presence of cycloheximide and accumulation of negative strand MHV RNA. *Virus Res.* **6,** 261–272.

PERLMAN, S., SCHELPER, R., BOLGER, E., and RIES, D. (1987). Late onset, symptomatic, demyelinating encephalomyelitis in mice infected with MHV-JHM in the presence of maternal antibody. *Microbiol. Pathol.* **2,** 185–194.

PICKEL, K., MULLER, M. A., and TER MEULEN, V. (1985). Influence of maternal immunity on the outcome of murine coronavirus JHM infection in suckling mice. *Med. Microbiol. Immunol.* **174,** 15–24.

SHEPHERD, A. M., PERKINS, W. J., GREEN, R. J., and CLARK, S. A. (1984). A study of oesophageal structure in a nematode, *Aphelenchiodes blastrophthorus* (Aphelenchida), using computer graphics reconstruction from serial thin sections. *J. Zool.* **204,** 271–288.

SIDDELL, S., WEGE, H., and TER MEULEN, V. (1983). The biology of coronaviruses. *J. Gen. Virol.* **64,** 761–776.

SORENSEN, O., PERRY, D., and DALES, S. (1980). *In vivo* and *in vitro* models of demyelinating diseases. III. JHM virus infection of rats. *Arch. Neurol.* **37,** 478–484.

STOHLMAN, S. A., and WEINER, L. P. (1981). Chronic central nervous system demyelination in mice after JHM virus infection. *Neurology* **31,** 38–44.

WEINER, L. P. (1973). Pathogenesis of demyelination induced by a mouse hepatitis virus. *Arch. Neurol.* **28,** 298–303.